Systems & Control Letters 135 (2020) 104586

Contents lists available at ScienceDirect

Systems & Control Letters

journal homepage: www.elsevier.com/locate/sysconle

Boundary observers for coupled diffusion–reaction systems with prescribed convergence rate

Leobardo Camacho-Solorio [a,*], Rafael Vazquez [b], Miroslav Krstic [a]

[a] Department of Mechanical and Aerospace Engineering, University of California San Diego, La Jolla, CA 92093-0411, United States of America
[b] Department of Aerospace Engineering, Universidad de Sevilla, Camino de los Descubrimiento s.n., 41092 Sevilla, Spain

ARTICLE INFO

Article history:
Received 17 May 2019
Received in revised form 24 September 2019
Accepted 18 October 2019
Available online xxxx

Keywords:
Boundary observer
State estimation
Partial differential equations

ABSTRACT

Following recent results on the boundary stabilization of coupled first-order hyperbolic equations by means of integral transformations, here a new result is presented for the problem of state estimation of coupled linear reaction–diffusion PDEs with Neumann boundary conditions from boundary measurements. For this purpose, an observer is constructed with a prescribed convergence rate. The stability of the estimation error system is derived by mapping the estimation error system to a stable target system using a pair of integral transformations. Our method is applicable as well to the dual problem of boundary stabilization of coupled linear reaction–diffusion PDEs. A numerical scheme, based on power series approximations of the kernels is formulated, taking into account the fact that the kernels are only piecewise differentiable.

1. Introduction

The problems of stabilization and estimation for coupled linear parabolic equations have been addressed recently, by means of the backstepping method for PDEs [1], in a series of publications. First, the stabilization and estimation problems for coupled reaction–diffusion equations, with constant parameters and equal diffusion coefficients, were solved in [2,3] and [4]. The extension to allow distinct diffusion coefficients was proposed later for coupled reaction–diffusion equations with constant coefficients in [5,6]. Then, boundary stabilization for coupled reaction–diffusion equations, with a spatially varying reaction, was solved in [7], in a relative general way. The generality allowed for subsequent results on the boundary estimation of coupled reaction–diffusion equations, with a spatially varying reaction, in [8], and on the boundary stabilization problem for coupled reaction–advection–diffusion equations with spatial variation in all parameters in [9]. Likewise, the problem of boundary stabilization and output regulation for one-dimensional coupled parabolic PIDEs with spatially varying coefficients and with Dirichlet, Neumann, and Robin boundary conditions was addressed in [10] and in [11], respectively. More recently, stabilization for a pair of coupled diffusion–reaction equations with unknown parameters was studied in [12]. The estimation and stabilization problems are closely related. In the estimation problem, one commonly designs an observer which guarantees some stability property for the origin of the estimation error system. The stability of the estimation error system then implies the convergence of the state estimate to the unknown state.

Briefly speaking, in the backstepping method, one seeks for an invertible transformation to map a, possibly unstable, PDE to a carefully selected stable *target* system. The transformation is typically an integral transformation and the main difficulty arises when trying to solve the PDEs verified by the kernels in the integral transformation. In [7,9] Volterra integral transformation (of second kind) was employed for a system of n coupled (advection)-reaction–diffusion equations. The kernels in [7,9] satisfy n^2 coupled second-order hyperbolic equations in a triangular domain and were solved by deriving an equivalent system of $2n^2$ coupled first-order hyperbolic equations, noticing a resemblance with the kernel equations appearing in the boundary stabilization problem of coupled systems of first-order hyperbolic equations [13,14]. A similar approach was followed in [8], but making use of a more recent solution of the boundary stabilization problems of coupled systems of first-order hyperbolic equations [15].

1.1. Contribution

The contribution of this paper is twofold, we provide a pair of integral transformations to decoupled the equation in the estimation error system and device a numerical method to compute the kernel equations.

First, motivated again by advances on the problem of boundary stabilization for coupled first-order hyperbolic equations [16]

* Corresponding author.
E-mail addresses: lcamacho@ucsd.edu (L. Camacho-Solorio), rvazquez1@us.es (R. Vazquez), krstic@ucsd.edu (M. Krstic).

https://doi.org/10.1016/j.sysconle.2019.104586
0167-6911/

where a decoupling technique is applied, we propose a new solution to the state estimation problem for coupled reaction–diffusion equations from boundary measurements. We show that a pair of integral transformations allows us to map the estimation error system into a simple stable *target* system, with uncoupled equations. Previous methods [5–11] lead to *target* systems with coupled equations, convoluting the assignment of an exact convergence rate or the formulation of robustness with respect to measurement disturbances [17]. Compared with [2–4], the result in this paper is not restricted to systems with equal diffusivity. The case with equal diffusion coefficients is less involved; in particular, a solution to the kernel equations can be found following the same method used in the problems with a single PDE. The result in this paper is not restricted to the problem of state estimation from boundary measurements. Actually, due to the similarity of the kernel equations in the problems of boundary stabilization and boundary estimation, this result is also applicable to problem of boundary stabilization of coupled linear reaction–diffusion PDEs. We derive and solve the equations for the kernels of each transformation; the first one over a triangular domain and the second one over a square of unit area. The solutions are constructed by the method of characteristics; where nontrivial partitions of the domains are required. We show that for both transformations, the kernel equations are second-order coupled hyperbolic, with a coupling between some of the kernels at the boundaries.

Second, we provide a simple numerical method to solve the kernel equations. The numerical scheme is based on polynomial approximations of the kernels; taking into account the fact that the kernels are piecewise differentiable. The problem of approximating solution of kernel equations by polynomials was studied previously in [18], where the authors formulate the approximation problem as an optimization problem, but it has not been applied to kernels with discontinuous derivatives.

1.2. Outline

The structure of the paper is as follows. In Section 2 the estimation problem is introduced. The main result in presented in Section 3. The solution to the kernel equations is derived in Section 4. A numerical scheme to compute the kernels is presented in Section 5; together with an example of the numerical computation 6. Finally, we conclude the paper with some remarks in Section 7.

2. Problem statement

2.1. Notation

- For a function $f : [0, 1] \mapsto \mathbb{R}^n$, with $f(x) = [f_1(x), \ldots, f_n(x)]^T$, such that $f_i \in \mathcal{L}^2(0, 1)$, for $i \in \{1, \ldots, n\}$, we use the following norm notation

$$\|f\|^2_{\mathcal{L}^2} = \int_0^1 |f(x)|_2^2 dx, \quad |f(x)|_2^2 = \sum_{i=1}^{n} |f_i(x)|^2, \tag{1}$$

- A function $f : [0, 1] \mapsto \mathbb{R}^n$ belong to the space $\mathcal{L}^2(0, 1; \mathbb{R}^n)$ if

$$\|f\|_{\mathcal{L}^2} < \infty, \tag{2}$$

2.2. Coupled parabolic reaction diffusion systems

Consider a linear reaction diffusion equation

$$u_t(x, t) = \Sigma u_{xx}(x, t) + \Lambda(x) u(x, t), \tag{3}$$

with coefficients

$$\Sigma = \begin{bmatrix} \epsilon_1 & \cdots & 0 \\ \vdots & \ddots & \vdots \\ 0 & \cdots & \epsilon_n \end{bmatrix}, \Lambda(x) = \begin{bmatrix} \lambda_{11}(x) & \cdots & \lambda_{1n}(x) \\ \vdots & \ddots & \vdots \\ \lambda_{n1}(x) & \cdots & \lambda_{nn}(x) \end{bmatrix}. \tag{4}$$

for $x \in (0, 1)$, $t \in (0, T]$, with $\lambda_{ij} \in C^1(0, 1)$ for all $i, j \in \{1, 2, \ldots, n\}$ and distinct diffusivities $\epsilon_i > 0$, for all $i \in \{1, 2, \ldots, n\}$. The state $u(x, t) \in \mathbb{R}^n$ is defined as

$$u(x, t) = [u_1(x, t), u_2(x, t), \ldots, u_n(x, t)]^T. \tag{5}$$

The boundary conditions are of Neumann type

$$u_x(0, t) = f_0(t), \quad u_x(1, t) = f_1(t) + Au(1, t), \tag{6}$$

and initial conditions $u_0 \in \mathcal{L}^2(0, 1)$, and $A_1 \in \mathbb{R}^{n\times n}$. The states are ordered so that $\epsilon_n > \cdots > \epsilon_2 > \epsilon_1 > 0$. The well-posedness of the system follows from standard results on linear parabolic equations [19, Subsection 7.1.3], [20]. In particular, we consider solutions which, as functions of the spatial variable, belong to the space $\mathcal{L}^2(0, 1)$. Eq. (3) and boundary conditions (6) constitute a dynamic system with state $u \in \mathcal{C}\left([0, T]; \mathcal{L}^2(0, 1)\right)$, known inputs $f_0 \in \mathcal{L}^2([0, T])$, $f_1 \in \mathcal{L}^2([0, T])$, and output measurement $y \in \mathcal{L}([0, t])$, with $y(t) = u(1, t)$. The estimation problem is to obtain an estimate $\widehat{u}$ of u, from boundary measurements f_0, f_1 and y. A boundary observer that provides a solution to this problem, with prescribed convergence rate, is provided in the next section.

Remark 1. The diffusion of lithium ions in the porous electrodes of lithium-ion batteries (with multiple active materials), is described by a system of (radial) diffusion equations, i.e., a system with $\Lambda = 0$, with a nonlinear coupling at the boundary. Linearization of the boundary coupling results in a boundary condition of the form (6), where $f_1(t)$ is related to the charge (or discharge) current, the matrix A relates the flux lithium ions in all the materials within the electrode to satisfy a potential equilibrium assumption.

2.3. Observer and estimation error systems

The proposed state observer is a copy of the reaction–diffusion system (3) with boundary conditions (6) together with boundary output error feedback

$$\widehat{u}_t(x, t) = \Sigma \widehat{u}_{xx}(x, t) + \Lambda(x)\widehat{u}(x, t) + P(x)\left[u(1, t) - \widehat{u}(1, t)\right] \tag{7}$$

for $x \in (0, 1)$, $t \in (0, T]$, with boundary conditions

$$\widehat{u}_x(0, t) = f_0(t), \tag{8}$$

$$\widehat{u}_x(1, t) = f_1(t) + Au(1, t) + Q\left[u(1, t) - \widehat{u}(1, t)\right], \tag{9}$$

and initial conditions $\widehat{u}_0 \in \mathcal{L}^2(0, 1)$. The observer state is $\widehat{u} \in \mathcal{C}([0, T]; \mathcal{L})$ and $u(1, t) - \widehat{u}(1, t)$ is the boundary output error. Observer gains $P(x)$ and Q are yet to be chosen. The estimation error system can be found by subtracting (7), (9) from (3), (6), to obtain

$$\widetilde{u}_t(x, t) = \Sigma \widetilde{u}_{xx}(x, t) + \Lambda(x)\widetilde{u}(x, t) - P(x)\widetilde{u}(1, t), \tag{10}$$

$$\widetilde{u}_x(0, t) = 0, \quad \widetilde{u}_x(1, t) = -Q\widetilde{u}(1, t), \tag{11}$$

where $\widetilde{u}(x,t) = u(x,t) - \widehat{u}(x,t)$, is the estimation error. The problem is then to find observer gains $P(x)$ and Q that guarantee exponential stability of the estimation error system

$$P(x) = -K(x,1)\Sigma B - K_s(x,1)\Sigma, \tag{12}$$
$$Q = B - K(1,1), \tag{13}$$

where the matrix $K(x,s) \in \mathbb{R}^{n\times n}$ is a solution of the following hyperbolic system of PDEs

$$\Sigma K_{xx} - K_{ss}\Sigma = -KC - \Lambda(x)K, \tag{14}$$

in the domain $\mathcal{T} = \{(x,s) : 0 < x < s < 1\}$ with boundary conditions

$$0 = K(x,x)\Sigma - \Sigma K(x,x), \tag{15}$$
$$\Lambda(x) + C = -\Sigma K_x(x,x) - K_s(x,x)\Sigma - \Sigma\frac{d}{dx}[K(x,x)], \tag{16}$$
$$H(s) = K_x(0,s), \tag{17}$$
$$0 = K(0,0), \tag{18}$$

where B and C are user defined diagonal matrices; with diagonal entries $b_1, b_2, \ldots, b_n \geq 0$ and $c_1, c_2, \ldots, c_n > 0$. The matrix $H(s)$ in (17) is lower triangular, that is $h_{ij} = 0$ if $j \geq i$. Each non-zero element $h_{ij}(s)$ is defined piecewise

$$h_{ij}(s) = \begin{cases} K_x^{ij}(0,s) & \text{for} \quad 0 \leq s \leq 1 - \sqrt{\frac{\epsilon_j}{\epsilon_i}}, \\ \check{K}_x^{ij}(0,s) & \text{for} \quad 1 - \sqrt{\frac{\epsilon_j}{\epsilon_i}} \leq s \leq 1, \end{cases} \tag{19}$$

and the matrix $\check{K}(x,s)$ is a solution of a second hyperbolic system of PDEs

$$\Sigma\check{K}_{xx} - \check{K}_{ss}\Sigma = C\check{K} - \check{K}C \tag{20}$$

defined in the square $\mathcal{S} = \{(x,s) : 0 < x < 1, 0 < s < 1\}$ with boundary conditions

$$\check{K}_s(x,1) = \check{K}_s(x,0) = \check{K}_x(1,s) = \check{K}(x,0) = 0, \tag{21}$$
$$\check{K}_x(0,s) = H(s). \tag{22}$$

The main results in the paper, stated in the next theorem, provide a solution to the estimation problem.

3. Stability of the estimation error system

Theorem 1. *The origin of the estimation error system (10)–(11), with initial condition $\widetilde{u}_0 \in \mathcal{L}^2(0,1)$ and observer gains computed from (13), is exponentially stable, that is, for any prescribed $\sigma > 0$, there exists a positive constant κ, such that*

$$\left\|\tilde{u}(\cdot,t)\right\|_{\mathcal{L}^2} \leq \kappa\exp[-\sigma t], \tag{23}$$

for all $t > 0$.

In the proof of Theorem 1, the main question is if the kernel PDEs (14)–(18) and (20)–(22) do indeed have a solution, as implicitly assumed in the theorem's statement, The next result answers this question.

Theorem 2. *Both systems of kernel equations (14)–(18) and (20)–(22) possess a continuous piecewise differentiable solution, $K(x,s)$ and $\check{K}(x,s)$, in their respective domains of definition, $\mathcal{T}$ and $\mathcal{S}$. In addition, the transformations T, $\check{T}$ defined by*

$$T[f](x) = f(x) - \int_x^1 K(x,s)f(s)ds, \tag{24}$$
$$\check{T}[f](x) = f(x) - \int_0^1 \check{K}(x,s)f(s)ds, \tag{25}$$

are invertible and both, the transformations and their inverses T^{-1} and $\check{T}^{-1}$, map $\mathcal{L}^2(0,1)$ functions into $\mathcal{L}^2(0,1)$ functions, verifying

$$k_1\|f\|_{\mathcal{L}^2} \leq \|T[f]\|_{\mathcal{L}^2} \leq k_2\|f\|_{\mathcal{L}^2}, \tag{26}$$
$$k_3\|f\|_{\mathcal{L}^2} \leq \|\check{T}[f]\|_{\mathcal{L}^2} \leq k_4\|f\|_{\mathcal{L}^2}. \tag{27}$$

for some $k_1, k_2, k_3, k_4 > 0$

The proof of Theorem 1 is presented in Section 3.2 and the proof of Theorem 2 is delivered in Section 4.

3.1. Target system

To prove that the choice of $P(x)$ and Q in (13) the origin of the estimation error system is exponentially stable two integral transformations are employed. The first transformation defined in (31), maps the estimation error system (10)–(11) to a first target system (28)–(29). The first transformation is a second-kind Volterra integral transformation, and alone, it will map the estimation error system to a target system with coupled boundary conditions along with set of kernel equations with some arbitrary terms in the boundary conditions [9]. Here, the first target system includes a boundary feedback term $\mathcal{H} : \mathcal{L}^2(0,1) \mapsto \mathbb{R}$, defined precisely such that a second transformation (32) exists, which will map the first target system (28)–(29) to a set of n uncoupled and stable diffusion reaction equations (33)–(34) and the kernel systems for both transformations include no arbitrary terms. The first target system is

$$w_t(x,t) = \Sigma w_{xx}(x,t) - Cw(x,t), \tag{28}$$

for $x \in (0,1)$, $t \in (0,T]$, with target state $w(x,t) = [w_1(x,t), \ldots, w_n(x,t)]^T$, and boundary conditions

$$w_x(0,t) = \mathcal{H}[w](x,t), \quad w_x(1,t) = -Bw(1,t). \tag{29}$$

In (28), matrices B and C are user-defined diagonal matrices. The term $\mathcal{H}$ in (29) is a linear bounded operator acting on the state w and applied in the boundary as feedback. The operator $\mathcal{H}$ has the form

$$\mathcal{H}[w](t) = \int_0^1 H(s)w(s,t)ds. \tag{30}$$

The matrix $H(s)$ is lower triangular, with non-zero entries defined in the transformation $T : \mathcal{L}^2(0,1) \to \mathcal{L}^2(0,1)$ that maps the first target system into the estimation error system is defined as

$$\widetilde{u}(x,t) = T[w](x,t) = w(x,t) - \int_x^1 K(x,s)w(s,t)ds, \tag{31}$$

where the kernel matrix $K(x,s)$ has entries denoted as $K^{ij}(x,s)$. The second transformation $\check{T} : \mathcal{L}^2(0,1) \to \mathcal{L}^2(0,1)$ is

$$v(x,t) = \check{T}[w](x,t) = w(x,t) - \int_0^1 \check{K}(x,s)w(s,t)ds, \tag{32}$$

where $\check{K}(x,s)$ is a lower triangular matrix, that is $\check{K}^{ij}(x,s) = 0$ if $j \geq i$, which maps the second target system into the first target system. The second target system is

$$v_t(x,t) = \Sigma v_{xx}(x,t) - Cv(x,t), \tag{33}$$

with boundary conditions

$$v_x(0,t) = 0, \quad v_x(1,t) = -Bv(1,t). \tag{34}$$

The pair of transformation is summarized conceptually in Fig. 1. Now, we prove the stability property needed for the second target system.

Fig. 1. Maps between the estimation error systems and the first and second target systems.

Proposition 3. *The origin $v \equiv 0$ of the system (33) with boundary conditions (34), and initial conditions $v_0 \in \mathcal{L}^2(0, 1)$ is exponentially stable in the $\mathcal{L}^2$ norm.*

Proof. The stability of the system (33)–(34), can be verified with the Lyapunov functional

$$V(t) = \frac{1}{2}\int_0^1 v(x,t)^T v(x,t)dx. \tag{35}$$

Taking the time derivate of $V(t)$ along the solutions of (33)–(34), and applying integrations by parts twice lets to

$$\frac{dV}{dt}(t) = -\sum_{i=1}^{n}\epsilon_i\left(b_i v(1,t)^2 + \int_0^1\left(\frac{\partial v_i}{\partial x}(x,t)\right)^2 dx\right) \tag{36}$$

$$= -\sum_{i=1}^{n} c_i\int_0^1 v_i(x,t)^2 dx, \tag{37}$$

For each $i \in \{1, \dots, n\}$, Wirtinger's inequality implies

$$\int_0^1 (v_i(x,t) - v_i(1,t))^2\, dx \le \frac{4}{\pi^2}\int_0^1\left(\frac{\partial v_i}{\partial x}(x,t)\right)^2 dx, \tag{38}$$

Then, using Young's inequality in the left hand side of (38) results in

$$\frac{\gamma}{\gamma+1}\int_0^1 v_i(x,t)^2 dx - \gamma v_i^2(1,t) \le \frac{4}{\pi^2}\int_0^1\left(\frac{\partial v_i}{\partial x}(x,t)\right)^2 dx, \tag{39}$$

for any $\gamma > 0$. In particular, by choosing $\gamma = 4b_i/\pi^2$, the inequalities in (39) become

$$\frac{\pi^2 b_i}{\pi^2+4b_i}\int_0^1 v_i(x,t)^2 dx \le b_i v_i^2(1,t) + \int_0^1\left(\frac{\partial v_i}{\partial x}(x,t)\right)^2 dx. \tag{40}$$

Substituting (40) into (36) lets to

$$\frac{dV}{dt}(t) \le -\sum_{i=1}^{n}\left(\epsilon_i\frac{\pi^2 b_i}{\pi^2+4b_i} + c_i\right)\int_0^1 v_i(x,t)^2 dx, \tag{41}$$

therefore

$$\frac{dV}{dt}(t) \le -2\sigma V(t),\ \text{with } \sigma = \min_{i\in\{1,\dots,n\}}\left\{\frac{\epsilon_i\pi^2 b_i}{\pi^2+4b_i} + c_i\right\}. \tag{42}$$

Finally, by the comparison principle

$$\|v(\cdot,t)\|_{\mathcal{L}^2} \le \|v_0\|_{\mathcal{L}^2}\exp\left[-\sigma t\right]. \quad \square \tag{43}$$

3.2. Proof of Theorem 1

Proof. Assume for the moment that Theorem 2 holds and that there is a solution to both kernel systems, (14)–(18) and (20)–(22), such that the transformations T and $\check{T}$ are invertible and both, transformations and their inverses, map $\mathcal{L}^2(0, 1)$ functions into $\mathcal{L}^2(0, 1)$ functions. Consider now the second target system in (33)–(34), with initial conditions $v_0(x)$ given by applying $\check{T}^{-1}$ to the initial condition of the first target system $w_0(x)$, that is

$$v_0(x) = \check{T}^{-1}\left[w_0\right](x) = w_0(x) - \int_0^1 \check{I}(x,s)w_0(s)ds, \tag{44}$$

where $\check{I}(x, s)$ is the kernel of the inverse transformation. Assume for that $w_0 \in \mathcal{L}^2(0, 1)$, thus have $v_0 \in \mathcal{L}^2(0, 1)$, and

$$\|w(\cdot,t)\|_2 \le \frac{k_3}{k_4}\|w_0\|_2\exp\left[-\sigma t\right]. \tag{45}$$

Consider now the first target system in (28)–(29), with initial conditions $w_0(x)$ given by applying T^{-1} to $\tilde{u}_0(x)$, that is

$$w_0(x) = T^{-1}\left[\tilde{u}_0\right](x) = \tilde{u}_0(x) - \int_0^1 I(x,s)\tilde{u}_0(s)ds, \tag{46}$$

where $\check{I}(x, s)$ is the kernel of the inverse transformation. Since $u_0 \in \mathcal{L}^2(0, 1)$, we do have $w_0 \in \mathcal{L}^2(0, 1)$, and from (45), it follows that

$$\|\tilde{u}(\cdot,t)\|_2 \le \frac{k_1k_3}{k_2k_4}\|\tilde{u}_0\|_2\exp\left[-\sigma t\right], \tag{47}$$

and Theorem 1 is proved. $\square$

In the next section, we construct the solution to both kernel systems and verify the invertibility of both transformations. The result is the proof for Theorem 2.

Remark 2. The well-posedness of the second target system (33)–(34) follows also from standard results on linear parabolic equations. This, along with the fact that transformations T and $\check{T}$ (and their inverses) map functions in $\mathcal{L}^2(0, 1)$ to $\mathcal{L}^2(0, 1)$, results in the well-posedness of observer system (7)–(8). In particular, we consider solutions $\widehat{u}(x, t)$ which, as functions of the spatial variable, belong to the space $\mathcal{L}^2(0, 1)$.

4. Solution to the kernel equations

4.1. Kernel equations for first transformation

The coefficients in the diagonal of $K(x, s)$ satisfy the equation

$$\epsilon_i K^{ii}_{xx}(x,s) - \epsilon_i K^{ii}_{ss}(x,s) = -c_i K^{ii}(x,s) - \sum_{l=1}^{l=n}\lambda_{il}(x)K^{li}(x,s), \tag{48}$$

for $i \in \{1, 2, \dots, n\}$, with boundary conditions

$$\frac{d}{dx}\left[K^{ii}(x,x)\right] = -\frac{c_i + \lambda_{ii}(x)}{2\epsilon_i}, \tag{49}$$

$$K^{ii}_x(0,s) = 0, \quad K^{ii}(0,0) = 0. \tag{50}$$

The coefficients in the upper triangular part of $K(x, s)$ satisfy the equation

$$\epsilon_i K^{ij}_{xx}(x,s) - \epsilon_j K^{ij}_{ss}(x,s) = -c_j K^{ij}(x,s) - \sum_{l=1}^{l=n}\lambda_{il}(x)K^{lj}(x,s), \tag{51}$$

for $i \in \{1, 2, \dots, n-1\}$ and $i < j$, with boundary conditions

$$K^{ij}_x(x,x) = \frac{\lambda_{ij}(x)}{\epsilon_j - \epsilon_i}, \quad K^{ij}_s(x,x) = \frac{\lambda_{ij}(x)}{\epsilon_i - \epsilon_j}, \tag{52}$$

$$K^{ij}(x,x) = 0, \quad K^{ij}_x(0,s) = 0, \quad K^{ij}(0,0) = 0. \tag{53}$$

The coefficients in the lower triangular part of $K(x, s)$ satisfy the equation

$$\epsilon_i K^{ij}_{xx}(x,s) - \epsilon_j K^{ij}_{ss}(x,s) = -c_j K^{ij}(x,s) - \sum_{l=1}^{l=n}\lambda_{il}(x)K^{lj}(x,s), \tag{54}$$

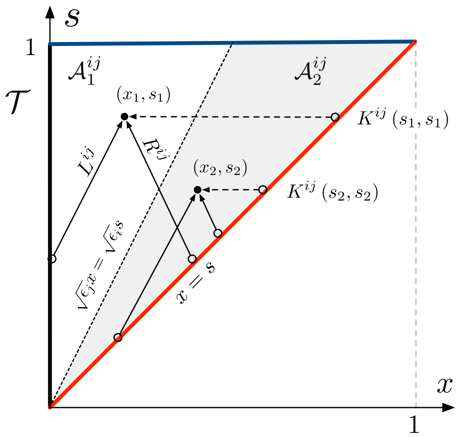

Fig. 2. Domain, boundary and characteristic lines for the upper diagonal coefficients of matrices $L(x, s)$ and $R(x, s)$.

for $i \in \{2, 3, \dots, n\}$ and $j < i$, with boundary conditions

$$K_x^{ij}(x,x) = \frac{\lambda_{ij}(x)}{\epsilon_j - \epsilon_i}, \quad K_s^{ij}(x,x) = \frac{\lambda_{ij}(x)}{\epsilon_i - \epsilon_j}, \tag{55}$$

$$K^{ij}(x,x) = 0, \quad K_x^{ij}(0,s) = h_{ij}(s), \quad K^{ij}(0,0) = 0. \tag{56}$$

4.2. Well posedness of kernel equations in first transformation

Lemma 4. *Assume each $h_{ij}(s)$ is known, bounded and continuous along the segment $1 - \sqrt{\epsilon_j/\epsilon_i} \le s \le 1$. Then, there exists a unique solution $K(x, s)$, satisfying Eq. (14) with boundary conditions (15)–(18). The solution is continuous and piecewise differentiable.*

Proof. Define auxiliary variables $L(x, s)$ and $R(x, s)$ as follows

$$L(x,s) = \sqrt{\Sigma}K_x(x,s) - K_s(x,s)\sqrt{\Sigma}, \tag{57}$$

$$R(x,s) = \sqrt{\Sigma}K_x(x,s) + K_s(x,s)\sqrt{\Sigma}. \tag{58}$$

Then, replacing (57) and (58) in (14) we obtain

$$\sqrt{\Sigma}L_x + L_s\sqrt{\Sigma} = -KC - \Lambda(x)K, \tag{59}$$

$$\sqrt{\Sigma}R_x - R_s\sqrt{\Sigma} = -KC - \Lambda(x)K. \tag{60}$$

Boundary conditions for (59) and (60) can be derived by substituting (57) and (58) in (15)–(18). The fact that $K(x, s)$ still appears on the right hand side of Eqs. (59) and (60) is not a problem since $K(x, s)$ can computed from $L(x, s)$ and $R(x, s)$ integrating (57) and (58) along horizontal lines and using the known values of $K(x, s)$ in the diagonal, that is

$$K^{ij}(x,s) = K^{ij}(s,s) - \frac{1}{2\sqrt{\epsilon_i}}\int_x^s \left[R^{ij}(z,s) + L^{ij}(z,s)\right] dz, \tag{61}$$

Eqs. (59) and (60) are analog to those found in [15,16]. The classification introduced for the elements of $K(x, s)$ remains unchanged after the change of variables and is useful to construct a solution for (59) and (60) using the method of characteristics. The diagonal coefficients of $L(x, s)$ and $R(x, s)$ satisfy the equations

$$\sqrt{\epsilon_i}L_x^{ii}(x,s) + \sqrt{\epsilon_i}L_s^{ii}(x,s) = -c_iK^{ii}(x,s) - \sum_{l=1}^{l=n}\lambda_{il}(x)K^{li}(x,s), \tag{62}$$

$$\sqrt{\epsilon_i}R_x^{ii}(x,s) - \sqrt{\epsilon_i}R_s^{ii}(x,s) = -c_iK^{ii}(x,s) - \sum_{l=1}^{l=n}\lambda_{il}(x)K^{li}(x,s), \tag{63}$$

for $i \in \{1, 2, \dots, n\}$, with boundary conditions

$$L^{ii}(0,s) = -R^{ii}(0,s), \tag{64}$$

$$R^{ii}(x,x) = -\frac{c_i + \lambda_{ii}(x)}{\sqrt{\epsilon_i}}. \tag{65}$$

Eqs. (62) and (63) with boundary conditions (65), can be solved using the method of characteristics. That is, writing (62) and (63) as integral equations along the characteristic; straight lines with slope 1 for (62) and slope -1 for (63). The coefficients of the upper triangular part of matrices $L(x, s)$ and $R(x, s)$ satisfy the equations

$$\sqrt{\epsilon_i}L_x^{ij}(x,s) + \sqrt{\epsilon_j}L_s^{ij}(x,s) = -c_jK^{ij}(x,s) - \sum_{l=1}^{l=n}\lambda_{il}(x)K^{lj}(x,s), \tag{66}$$

$$\sqrt{\epsilon_i}R_x^{ij}(x,s) - \sqrt{\epsilon_j}R_s^{ij}(x,s) = -c_jK^{ij}(x,s) - \sum_{l=1}^{l=n}\lambda_{il}(x)K^{lj}(x,s), \tag{67}$$

for $i \in \{1, 2, \dots, n-1\}$, and $i < j$, with boundary conditions

$$L^{ij}(x,x) = \frac{\lambda_{ij}(x)}{\sqrt{\epsilon_j} - \sqrt{\epsilon_i}}, \quad L^{ij}(0,s) = -R^{ij}(0,s), \tag{68}$$

$$R^{ij}(x,x) = -\frac{\lambda_{ij}(x)}{\sqrt{\epsilon_i} + \sqrt{\epsilon_j}}. \tag{69}$$

Eqs. (66) and (67), with boundary conditions (68), (69), can be solved using the method of characteristics. That is, writing (66) and (67) as integral equations along the characteristic lines; straight lines with slope $\sqrt{\epsilon_j/\epsilon_i}$ for (66) and $-\sqrt{\epsilon_j/\epsilon_i}$ for (66). The boundary condition (69) provides enough information to solve for $R^{ij}(x, s)$ in the whole domain. However, to solve for $L^{ij}(x, s)$, boundary information from two segments of the boundary is needed. Specifically, to compute $L^{ij}(x, s)$ in the set $\mathcal{A}_1^{ij} = \{(x, s) \in \mathcal{T} : \sqrt{\epsilon_j}x \le \sqrt{\epsilon_i}s\}$, the boundary condition (68), given at the left side of the triangle ($x = 0$), is needed. On the other hand, to compute $L^{ij}(x, s)$ in the set $\mathcal{A}_2^{ij} = \{(x, s) \in \mathcal{T} : \sqrt{\epsilon_i}s \le \sqrt{\epsilon_j}x\}$, the boundary condition (68), given at the diagonal of the triangle ($x = s$), is needed. This results in a discontinuity for the function $L^{ij}(x, s)$ at the line $\sqrt{\epsilon_i}s = \sqrt{\epsilon_j}x$, but results only in a discontinuity for the first derivatives of the elements $K^{ij}(x, s)$, as can be seen from the definition (57). The geometry of the problem, that is, the characteristic lines, the boundary, and the partition of the domain in sets $\mathcal{A}_1^{ij}$ and $\mathcal{A}_2^{ij}$, is shown in Fig. 2. The coefficients in the lower triangular part of the matrices $L(x, s)$ and $R(x, s)$ satisfy the equations

$$\sqrt{\epsilon_i}L_x^{ij}(x,s) + \sqrt{\epsilon_j}L_s^{ij}(x,s) = -c_jK^{ij}(x,s) - \sum_{l=1}^{l=n}\lambda_{il}(x)K^{lj}(x,s), \tag{70}$$

$$\sqrt{\epsilon_i}R_x^{ij}(x,s) - \sqrt{\epsilon_j}R_s^{ij}(x,s) = -c_jK^{ij}(x,s) - \sum_{l=1}^{l=n}\lambda_{il}(x)K^{lj}(x,s), \tag{71}$$

for $i \in \{2, 3, \dots, n\}$ and $j < i$, with boundary conditions

$$L^{ij}(x,x) = \frac{\lambda_{ij}(x)}{\sqrt{\epsilon_j} - \sqrt{\epsilon_i}}, \tag{72}$$

and

$$L^{ij}(0,s) = 2\sqrt{\epsilon_i}h_{ij}(s) - R^{ij}(0,s), \tag{73}$$

$$R^{ij}(x,x) = -\frac{\lambda_{ij}(x)}{\sqrt{\epsilon_i} + \sqrt{\epsilon_j}}. \tag{74}$$

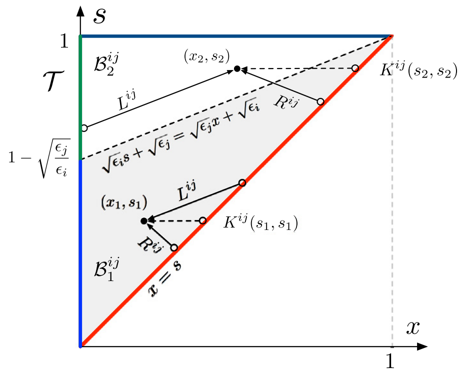

Fig. 3. Domain, boundary and characteristic lines for the lower diagonal coefficients of matrices $L(x, s)$ and $R(x, s)$.

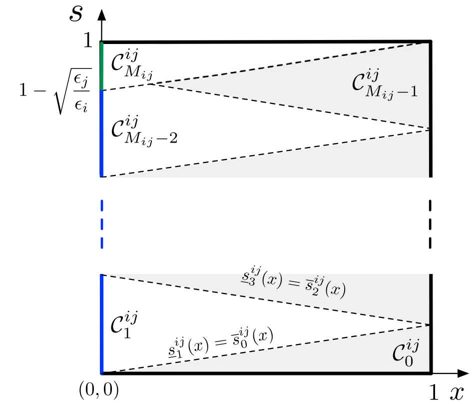

Fig. 4. Partition of the domain for the kernel in the second transformation.

Eqs. (70) and (71) with boundary conditions (72)–(74) can be solved using the method of characteristics. That is, writing (70) and (71) as integral equations along the characteristic lines. The characteristic lines are straight lines with slope $\sqrt{\epsilon_j/\epsilon_i}$ for (70) and $-\sqrt{\epsilon_j/\epsilon_i}$ for (71). Boundary condition (74) provides enough information to compute $R^{ij}(x, s)$ in the whole domain. Boundary conditions (72) at the diagonal ($x = s$) allow us to compute $L^{ij}(x, s)$ in the set $\mathcal{B}_1^{ij} = \{(x, s) \in \mathcal{T} : \sqrt{\epsilon_i}s + \sqrt{\epsilon_j} \leq \sqrt{\epsilon_j}x + \sqrt{\epsilon_i}\}$. The segment of the left boundary that coincides with the piece $\mathcal{B}_1^{ij}$ is precisely the segment where $h_{ij}(s)$ is defined in terms of $K_x(0, s)$; hence, avoiding inconsistency due to overdetermination. Boundary conditions (73) at the left side ($x = 0$), allow us to compute $L^{ij}(x, s)$ in the remaining set, that is, $\mathcal{B}_2^{ij} = \{(x, s) \in \mathcal{T} : \sqrt{\epsilon_j}x + \sqrt{\epsilon_i} \leq \sqrt{\epsilon_i}s + \sqrt{\epsilon_j}\}$. The segment of the left boundary that coincides with $\mathcal{B}_2^{ij}$ is precisely the segment where $h_{ij}(s)$ is defined in terms of $\check{K}_x(0, s)$. Thus, the piecewise definition of $h_{ij}(s)$ in (19) serves the double purpose of avoiding *overdetermination* and providing boundary conditions to avoid *underdetermination*. Again, there is a discontinuity in the function $L^{ij}(x, s)$ at the line $\sqrt{\epsilon_i}s + \sqrt{\epsilon_j} = \sqrt{\epsilon_j}x + \sqrt{\epsilon_i}$, but results only in a discontinuity for the first derivatives of the elements $K^{ij}(x, s)$, as can be seen from definition (57). The geometry of the problem, that is, the characteristic lines, the boundary, and the partition of the domain in sets $\mathcal{B}_1^{ij}$ and $\mathcal{B}_2^{ij}$, is shown in Fig. 3. Using the method of successive approximation, it can be verified that the integral equations for all the coefficients of $L(x, s)$ and $R(x, s)$ have a unique solution. Eq. (61) is then used to recover $K(x, s)$ from $L(x, s)$ and $R(x, s)$. □

Next, we construct a solution in the system (20)–(22).

4.3. Kernel equations for second transformation

For each coefficient $\check{K}^{ij}(x, s)$, we divide the domain in $M_{ij} + 1$ polygons (M_{ij} of which are triangles and 1 quadrilateral), with

$$M_{ij} = 2\left\lceil \frac{1}{2}\left(\sqrt{\frac{\epsilon_i}{\epsilon_j}} - 1\right)\right\rceil + 1, \tag{75}$$

where $\lceil \cdot \rceil$ stands for the ceiling function. We denote these polygons $\mathcal{C}_k^{ij}$; for $k \in \{0, 1, \dots, M_{ij}\}$. The sets $\mathcal{C}_0^{ij}$ and $\mathcal{C}_{M_{ij}}^{ij}$ are triangles defined as

$$\mathcal{C}_0^{ij} = \left\{(x, s) \in \mathcal{S} : 0 \leq s \leq \sqrt{\frac{\epsilon_j}{\epsilon_i}}x\right\}, \tag{76}$$

$$\mathcal{C}_{M_{ij}}^{ij} = \left\{(x, s) \in \mathcal{S} : 1 + (x - 1)\sqrt{\frac{\epsilon_j}{\epsilon_i}} \leq s \leq 1\right\}. \tag{77}$$

For $0 < k < M_{ij}$, the sets $\mathcal{C}_k^{ij}$ are polygons defined as

$$\mathcal{C}_k^{ij} := \left\{(x, s) \in \mathcal{S} : \underline{s}_k^{ij}(x) \leq s \leq \bar{s}_k^{ij}(x), \right.$$
$$\left. s \leq 1 + (x - 1)\sqrt{\frac{\epsilon_j}{\epsilon_i}}\right\}, \tag{78}$$

with

$$\underline{s}_k^{ij}(x) = \begin{cases} (k-1)\sqrt{\frac{\epsilon_j}{\epsilon_i}} + x\sqrt{\frac{\epsilon_j}{\epsilon_i}} & \text{for } k \text{ odd,} \\ k\sqrt{\frac{\epsilon_j}{\epsilon_i}} - x\sqrt{\frac{\epsilon_j}{\epsilon_i}} & \text{for } k \text{ even,} \end{cases} \tag{79}$$

$$\bar{s}_k^{ij}(x) = \begin{cases} (k+1)\sqrt{\frac{\epsilon_j}{\epsilon_i}} + x\sqrt{\frac{\epsilon_j}{\epsilon_i}} & \text{for } k \text{ odd,} \\ k\sqrt{\frac{\epsilon_j}{\epsilon_i}} + x\sqrt{\frac{\epsilon_j}{\epsilon_i}}, & \text{for } k \text{ even.} \end{cases} \tag{80}$$

Note that $S = \bigcup_{k=0}^{M_{ij}} \mathcal{C}_k^{ij}$; Fig. 4 shows this partition. In the triangle $\mathcal{C}_0^{ij}$, the element $\check{K}^{ij}(x, s)$ satisfies

$$\epsilon_i \check{K}_{xx}^{ij}(x, s) - \epsilon_j \check{K}_{ss}^{ij}(x, s) = [c_i - c_j]\check{K}^{ij}(x, s), \tag{81}$$

with boundary conditions

$$\check{K}^{ij}(x, 0) = \check{K}_s^{ij}(x, 0) = \check{K}_x^{ij}(1, s) = 0. \tag{82}$$

Thus, in the piece $\mathcal{C}_0^{ij}$, the unique solution is simply

$$\check{K}^{ij}(x, s) = 0. \tag{83}$$

For k odd and $0 < k < M_{ij}$, the sets $\mathcal{C}_k^{ij}$ are either triangles or a quadrilateral if $k = M_{ij} - 2$. In these sets the function $\check{K}^{ij}(x, s)$ satisfies the equation

$$\epsilon_i \check{K}_{xx}^{ij}(x, s) - \epsilon_j \check{K}_{ss}^{ij}(x, s) = [c_i - c_j]\check{K}^{ij}(x, s), \tag{84}$$

with a boundary condition

$$\check{K}_x^{ij}(0, s) = h_{ij}(s). \tag{85}$$

In addition, continuity at the intersection between $\mathcal{C}_k^{ij}$ and $\mathcal{C}_{k-1}^{ij}$ implies that $\check{K}^{ij}(x, s)$ is given along the segment defined by $\underline{s}_k^{ij}(x)$; assuming a unique solution has been found in the previous piece $\mathcal{C}_{k-1}^{ij}$.

For k even and $0 < k < M_{ij}$, the sets $\mathcal{C}_k^{ij}$ are all triangles, and in these sets the function $K^{ij}(x, s)$ satisfies the equation

$$\epsilon_i \check{K}_{xx}^{ij}(x, s) - \epsilon_j \check{K}_{ss}^{ij}(x, s) = [c_i - c_j]\check{K}^{ij}(x, s), \tag{86}$$

and a boundary condition

$$\check{K}_x^{ij}(0, s) = 0. \tag{87}$$

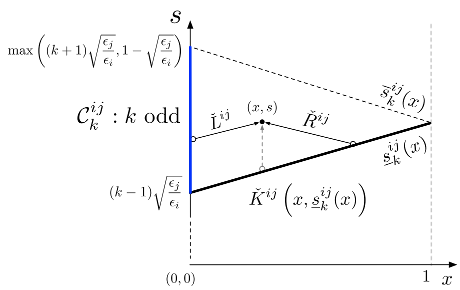

Fig. 5. Polygon $\mathcal{C}_k^{ij}$ for k odd.

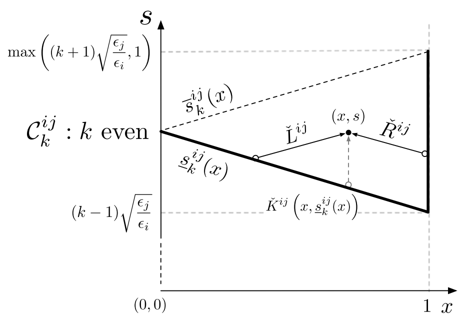

Fig. 6. Polygon $\mathcal{C}_k^{ij}$ for k even.

In addition, the continuity requirement at the intersection between $\mathcal{C}_k^{ij}$ and $\mathcal{C}_{k-1}^{ij}$ implies that $\check{K}^{ij}(x,s)$ is given along the segment defined by $\underline{s}_k^{ij}(x)$; assuming a unique solution has been found in the previous piece $\mathcal{C}_{k-1}^{ij}$.

Finally, in the triangle $\mathcal{C}_{M_{ij}}^{ij}$ the function $\check{K}^{ij}(x,s)$ satisfies

$$\epsilon_i \check{K}_{xx}^{ij}(x,s) - \epsilon_j \check{K}_{ss}^{ij}(x,s) = [c_i - c_j]\check{K}^{ij}(x,s), \tag{88}$$

with the boundary condition

$$\check{K}_s^{ij}(x,1) = 0. \tag{89}$$

In addition, the continuity requirement at the intersections between $\mathcal{C}_{M_{ij}}^{ij}$ and $\mathcal{C}_{M_{ij}-1}^{ij}$ and between $\mathcal{C}_{M_{ij}}^{ij}$ and $\mathcal{C}_{M_{ij}-2}^{ij}$ implies that $\check{K}^{ij}(x,s)$ is given along the segment defined by $s = 1+(x-1)\sqrt{\frac{\epsilon_j}{\epsilon_i}}$, from the assumption that a unique solution has been found in the previous set $\mathcal{C}_{M_{ij}-1}^{ij}$.

Note that finding the solution $\check{K}(x,s)$ at $\mathcal{C}_{M_{ij}}$ completes the piecewise definition of $H(s)$, i.e.

$$h_{ij}(s) = \begin{cases} K_x^{ij}(0,s) & \text{for } 0 \le s \le 1-\sqrt{\frac{\epsilon_j}{\epsilon_i}}, \\ \check{K}_x^{ij}(0,s) & \text{for } 1-\sqrt{\frac{\epsilon_j}{\epsilon_i}} \le s \le 1. \end{cases} \tag{90}$$

Therefore, the boundary condition used to solve system (14)–(18) is not longer arbitrary.

4.4. Well posedness of kernel equations in second transformation

Lemma 5. *If each $h_{ij}(0,s)$ is bounded and continuous on the segment $0 \le s \le 1-\sqrt{\epsilon_j/\epsilon_i}$, then there exists a unique solution $\check{K}^{ij}(x,s)$ satisfying Eq. (20) and boundary conditions (21)–(22). The solution is defined piecewise and is continuous over all the domain.*

Proof. Since the unique solution at $\mathcal{C}_0^{ij}$ is $\check{K}^{ij}(x,s) = 0$, to find a (continuous) solution in the whole domain, it is sufficient to prove that a unique solution can be found at $\mathcal{C}_k^{ij}$ given a solution in all previous sets $\mathcal{C}_{k-1}^{ij}, \mathcal{C}_{k-2}^{ij}, \dots, \mathcal{C}_0^{ij}$.

Define again auxiliary variables $\check{L}(x,s)$ and $\check{R}(x,s)$ as follows

$$\check{L}(x,s) = \sqrt{\Sigma}\check{K}_x(x,s) - \check{K}_s(x,s)\sqrt{\Sigma}, \tag{91}$$

$$\check{R}(x,s) = \sqrt{\Sigma}\check{K}_x(x,s) + \check{K}_s(x,s)\sqrt{\Sigma}. \tag{92}$$

In the case k is odd and $0 < k < M_{ij}$, the functions $\check{L}^{ij}(x,s)$ and $\check{R}^{ij}(x,s)$ satisfy the first order equations

$$\sqrt{\epsilon_i}\check{L}_x^{ij}(x,s) + \sqrt{\epsilon_j}\check{L}_s^{ij}(x,s) = \left[c_i - c_j\right]\check{K}^{ij}(x,s) \tag{93}$$

$$\sqrt{\epsilon_i}\check{R}_x^{ij}(x,s) - \sqrt{\epsilon_j}\check{R}_s^{ij}(x,s) = \left[c_i - c_j\right]\check{K}^{ij}(x,s) \tag{94}$$

with boundary conditions

$$\check{L}^{ij}(0,s) = 2\sqrt{\epsilon_i}h(s) - \check{R}^{ij}(0,s), \tag{95}$$

$$\check{R}^{ij}(x,\underline{s}_k^{ij}(x)) = \sqrt{\epsilon_i}\check{K}_x^{ij}\left(x,\underline{s}_k^{ij}(x)\right) + \sqrt{\epsilon_j}\check{K}_s^{ij}\left(x,\underline{s}_k^{ij}(x)\right). \tag{96}$$

The fact that there is a shared boundary between $\mathcal{C}_k^{ij}$ and $\mathcal{C}_{k-1}^{ij}$, i.e. $\underline{s}_k^{ij}(x) = \bar{s}_{k-1}^{ij}(x)$, and the assumption that $\check{K}^{ij}(x,s)$ is known at $\mathcal{C}_{k-1}^{ij}$, implies that the right hand side of (96) is known and bounded. Eqs. (93) and (94) with boundary conditions (95) and (96) can be solved using the method of characteristics. That is, writing (93) and (94) as integral equations along the characteristic lines. The characteristic lines are straight lines with slope $\sqrt{\epsilon_j/\epsilon_i}$ for (93) and $-\sqrt{\epsilon_j/\epsilon_i}$ for (94). The geometry of the problem, that is, the characteristic lines, the boundary, and the domain $\mathcal{C}_k^{ij}$ (for k odd and $0 < k < M_{ij}$) is depicted in Fig. 5.

In the case k is even and $0 < k < M_{ij}$, functions $\check{L}^{ij}(x,s)$ and $\check{R}^{ij}(x,s)$ satisfy the same first-order hyperbolic equations

$$\sqrt{\epsilon_i}\check{L}_x^{ij}(x,s) + \sqrt{\epsilon_j}\check{L}_s^{ij}(x,s) = \left[c_i - c_j\right]\check{K}^{ij}(x,s) \tag{97}$$

$$\sqrt{\epsilon_i}\check{R}_x^{ij}(x,s) - \sqrt{\epsilon_j}\check{R}_s^{ij}(x,s) = \left[c_i - c_j\right]\check{K}^{ij}(x,s) \tag{98}$$

with boundary conditions

$$\check{L}^{ij}(x,\underline{s}_k^{ij}(x)) = \sqrt{\epsilon_i}\check{K}_x^{ij}\left(x,\underline{s}_k^{ij}(x)\right) - \sqrt{\epsilon_j}\check{K}_s^{ij}\left(x,\underline{s}_k^{ij}(x)\right), \tag{99}$$

$$\check{R}^{ij}(1,s) = -\check{L}^{ij}(1,s). \tag{100}$$

The fact that there is a shared boundary between $\mathcal{C}_k^{ij}$ and $\mathcal{C}_{k-1}^{ij}$, i.e. $\underline{s}_k^{ij}(x) = \bar{s}_{k-1}^{ij}(x)$, and the assumption that $\check{K}^{ij}(x,s)$ is known at $\mathcal{C}_{k-1}^{ij}$, imply that the right hand side of (99) is known and bounded. Eqs. (97) and (98) with boundary conditions (99) and (100) can be solved using the method of characteristics. That is, writing (97) and (98) as integral equations along the characteristic lines. The characteristic lines are straight lines with slope $\sqrt{\epsilon_j/\epsilon_i}$ for (97) and $-\sqrt{\epsilon_j/\epsilon_i}$ for (98). The geometry of the problem, that is, the characteristic lines, the boundary, and the domain $\mathcal{C}_k^{ij}$ (for k even and $0 < k < M_{ij}$) is depicted in Fig. 6.

Finally, for $k = M_{ij}$, functions $\check{L}^{ij}(x,s)$ and $\check{R}^{ij}(x,s)$ satisfy the same first-order hyperbolic equations

$$\sqrt{\epsilon_i}\check{L}_x^{ij}(x,s) + \sqrt{\epsilon_j}\check{L}_s^{ij}(x,s) = \left[c_i - c_j\right]\check{K}^{ij}(x,s), \tag{101}$$

$$\sqrt{\epsilon_i}\check{R}_x^{ij}(x,s) - \sqrt{\epsilon_j}\check{R}_s^{ij}(x,s) = \left[c_i - c_j\right]\check{K}^{ij}(x,s), \tag{102}$$

and boundary conditions

$$\check{L}^{ij}(x,1) = \check{R}^{ij}(x,1), \tag{103}$$

$$\check{R}^{ij}\left(x, 1+(x-1)\sqrt{\frac{\epsilon_j}{\epsilon_i}}\right) = \sqrt{\epsilon_i}\check{K}_x^{ij}\left(x, 1+(x-1)\sqrt{\frac{\epsilon_j}{\epsilon_i}}\right) + \sqrt{\epsilon_j}\check{K}_s^{ij}\left(x, 1+(x-1)\sqrt{\frac{\epsilon_j}{\epsilon_i}}\right). \tag{104}$$

In this case, $\mathcal{C}_{M_{ij}}^{ij}$ shares a boundary with two previous sets: $\mathcal{C}_{M_{ij}-1}^{ij}$ and $\mathcal{C}_{M_{ij}-2}^{ij}$. The assumption that $\check{K}^{ij}(x,s)$ is known at $\mathcal{C}_{M_{ij}-1}^{ij}$,

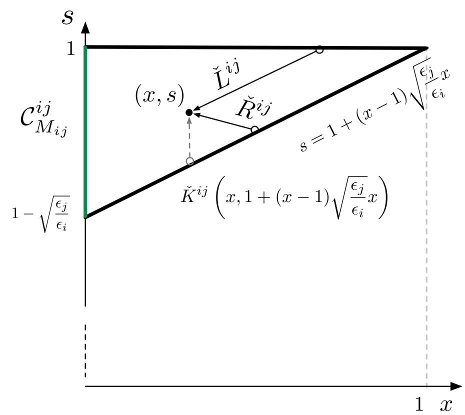

Fig. 7. Polygon $\mathcal{C}^{ij}_{M_{ij}}$. Note that solving $\check{K}^{ij}$ in section $\mathcal{C}^{ij}_{M_{ij}}$ provides the value of $h_{ij}(s)$ along the segment.

and $\mathcal{C}^{ij}_{M_{ij}-2}$, implies that the right hand side of (103) is known and bounded. Eqs. (101) and (102) with boundary conditions (103) and (104) can be solved using the method of characteristics. The characteristic lines are straight lines with slope $\sqrt{\epsilon_j/\epsilon_i}$ for Eq. (101) and $-\sqrt{\epsilon_j/\epsilon_i}$ for Eq. (102). The geometry of the problem, that is, the characteristic lines, the boundary, and the domain $\mathcal{C}^{ij}_{M_{ij}}$ is depicted in Fig. 7.

The fact that $\check{K}^{ij}(x,s)$ appears on the right hand side of the equations is not a problem, since for $0 < k < M_{ij}$

$$\check{K}^{ij}(x,s) = \check{K}^{ij}(x, \underline{s}^{ij}_k(x)) + \frac{1}{2\sqrt{\epsilon_j}} \int_{\underline{s}^{ij}_k(x)}^{s} \Big[\check{R}^{ij}(x,\xi) + \check{L}^{ij}(x,\xi)\Big] d\xi, \tag{105}$$

for $(x,s) \in \mathcal{A}^{ij}_k$. And, for $k = M_{ij}$

$$\check{K}^{ij}(x,s) = \check{K}^{ij}\left(x, 1+(x-1)\sqrt{\frac{\epsilon_j}{\epsilon_i}}\right) + \frac{1}{2\sqrt{\epsilon_j}} \int_{1+(x-1)\sqrt{\frac{\epsilon_j}{\epsilon_i}}}^{s} \Big[\check{R}^{ij}(x,\xi) + \check{L}^{ij}(x,\xi)\Big] d\xi, \tag{106}$$

for $(x,s) \in \mathcal{A}^{ij}_{M_{ij}}$. Using the method of successive approximations, it can be verified that the integral equations derived from the method of characteristics have a unique solution. Eqs. (105) and (106) are used to recover $\check{K}(x,s)$ from the solutions $\check{L}(x,s)$ and $\check{R}(x,s)$. □

Lemma 6. *There is a unique solution $K(x,s)$, $\check{K}(x,s)$ to Eqs. (14) and (20) with boundary conditions (15)–(18) and (21)–(22). The solution is defined piecewise and is continuous over all the domain*

Proof. The n elements in a given column $j \in \{1,2,\dots,n\}$ of $K(x,s)$ together with the $j-1$ non-zero elements in the same column j of $\check{K}(x,s)$ form a system that is independent of all other elements in both matrices. Thus, the problem can be solved in a column-wise fashion. In particular, for the last column, all elements of $\check{K}(x,s)$ are zero and the elements $K^{i,n}(x,s)$ for $i \in \{1,2,\dots,n\}$ can be solved following Lemma 4 without the need to solve for $\check{K}(x,s)$. For any other column $j \in \{1,2,\dots,n-1\}$, the problem can be solve sequentially as follows. For a fix column $j^\star \in \{1,2,\dots,n-1\}$, all elements $K^{i,j^\star}(x,s)$, $i \in \{1,2,\dots,n\}$ can be found in the subset $\mathcal{B}^{n,j^\star}_1$ (see Fig. 3), without need to solve for any element in $\check{K}^{i,j^\star}(x,s)$, following to Lemma 4. In particular, the solution $K^{n,j^\star}$, restricted to the subset $\mathcal{B}^{n,j^\star}_1$, provides the boundary conditions needed to solve for $\check{K}^{n,j^\star}(x,s)$, in its whole domain of definition $\mathcal{S}$, following Lemma 5. Since $\check{K}^{n,j^\star}(x,s)$ is available, one can solve for all elements $K^{ij^\star}(x,s)$, $i \in \{1,2,\dots,n\}$ in the subset $\mathcal{B}^{n-1,j^\star}_1$, following Lemma 4. In particular, the solution $\check{K}^{n,j^\star}$ restricted to the subset $\mathcal{B}^{n-1,j^\star}_1$ provides all information needed to solve for $\check{K}^{n-1,j^\star}(x,s)$ its whole domain of definition $\mathcal{S}$, following Lemma 5. Note that $\mathcal{B}^{n,j^\star}_1 \subset \mathcal{B}^{n-1,j^\star}_1 \subset \dots \subset \mathcal{B}^{1,j^\star}_1$. The procedure is repeated until the solution is found for all non zero terms $\check{K}^{i,j^\star}(x,s)$, $i \in \{1,2,\dots,j^\star-1\}$ in $\mathcal{S}$. Finally, the solution $\check{K}^{i,j^\star}(x,s)$, $i \in \{1,2,\dots,j^\star-1\}$ in $\mathcal{S}$, provides all the boundary conditions needed to compute $K^{i,j^\star}(x,s)$, $i \in \{1,2,\dots,n\}$ in $\mathcal{T}$. □

4.5. Inversion of the transformations

Lemma 7. *There exist integral transformations, mapping the function $\widetilde{u}$ to w, i.e. an inverse transformation of $\check{T}$, in the form*

$$w(x,t) = \check{T}^{-1}[\widetilde{u}](x,t) = \widetilde{u}(x,t) + \int_0^1 I(x,s)\widetilde{u}(s,t)ds, \tag{107}$$

Proof. The existence of an inverse transformation follows from the boundedness of the kernel $K(x,s)$ and known properties of second-kind Volterra integral equations. □

Lemma 8. *There exists an integral transformation, mapping the function w to v, i.e. an inverse transformation of $\check{T}$, in the form*

$$v(x,t) = \check{T}^{-1}[w](x,t) = w(x,t) + \int_0^1 \check{I}(x,s)w(s,t)ds, \tag{108}$$

Proof. The structure of $\check{K}(x,s)$ implies the invertibility of transformation $\check{T}$. This is verified with an induction argument by noticing that

$$v_1(x,t) = w_1(x,t), \tag{109}$$

and

$$v_i(x,t) = w_i(x,t) + \sum_{l=1}^{i-1} \int_0^1 \check{K}^{il}(x,s)w_l(s,t)ds. \tag{110}$$

for $i \in \{2,\dots,n\}$. The inverse has, in fact, the same structure as the direct transformation, that is

$$v(x,t) = \check{T}^{-1}[w](x,t) = w(x,t) + \int_0^1 \check{I}(x,s)w(s,t)ds, \tag{111}$$

where $\check{I}(x,s)$ is lower triangular, where each $\check{I}^{ij}(x,s)$ is simply computed from $\check{K}(x,s)$. □

5. A numerical method to compute kernels

The numerical approximation of the kernels is based on a piecewise polynomial approximation that takes into account the piecewise differential nature of the kernels. For the approximation of coefficients in $K(x,s)$, the domain is divided according to the intersection of the sets $\mathcal{A}^{ij}_1$, $\mathcal{A}^{ij}_2$, $\mathcal{B}^{ij}_1$ and $\mathcal{B}^{ij}_2$, defined in Section 4 (Figs. 2 and 3) corresponding to all the coefficients within the same column; due to the column-wise coupling in Eqs. (48), (51) and (54). For the approximation of coefficients in $\check{K}(x,s)$, the domain is divided according to the sets $\mathcal{C}^{ij}_k$ defined in Section 4 (Fig. 4), with an additional partition of the set $\mathcal{C}^{ij}_{M_{ij}}$. The extra partition is required since the boundary conditions at the diagonal side of $\mathcal{C}^{ij}_{M_{ij}}$ have a discontinuity, due to the fact that the diagonal side of $\mathcal{C}^{ij}_{M_{ij}}$ coincides with two other sets, $\mathcal{C}^{ij}_{M_{ij}-1}$

and $C^{ij}_{M_{ij}-2}$. For each coefficient in $K(x,s)$ or $\check{K}(x,s)$, an index $p \in \{1,\dots,p^{\max}\}$ is employed to indicate the polynomial approximation in a particular piece the domain $\mathcal{T}$ or $\mathcal{S}$. The numbers of pieces $p^{\max}$ is not the same for all coefficients. For the coefficient $\check{K}^{ij}(x,s)$, the number of pieces in the partition of $\mathcal{S}$ is

$$p^{\max} = \begin{cases} M_{ij}+2 & \text{if} \quad \lceil 1/2\left(\sqrt{\epsilon_i/\epsilon_j}-1\right)\rceil > 1/2\sqrt{\epsilon_i/\epsilon_j}, \\ M_{ij}+1 & \text{if} \quad \lceil 1/2\left(\sqrt{\epsilon_i/\epsilon_j}-1\right)\rceil < 1/2\sqrt{\epsilon_i/\epsilon_j}, \\ M_{ij} & \text{if} \quad \lceil 1/2\left(\sqrt{\epsilon_i/\epsilon_j}-1\right)\rceil = 1/2\sqrt{\epsilon_i/\epsilon_j}, \end{cases} \tag{112}$$

with M_{ij} defined in (75).

For each piece $p \in \{1,\dots,p^{max}\}$, the mth order *triangular* polynomial approximation of $K^{ij}(x,y)$ and $\check{K}^{ij}(x,y)$ has the form

$$_pK^{ij}_m(x,s) = \sum_{a=0}^{m}\sum_{b=0}^{m-a} {}_pd^{ij}_{ab}x^a s^b, \tag{113}$$

$$_p\check{K}^{ij}_m(x,s) = \sum_{a=0}^{m}\sum_{b=0}^{m-a} {}_p\check{d}^{ij}_{ab}x^a s^b, \tag{114}$$

where the values of coefficients ${}_pd^{ij}_{ab}, {}_p\check{d}^{ij}_{ab} \in \mathbb{R}$, are found from equations and boundary or continuity conditions. For the numerical approximation it is convenient to use the second-order hyperbolic equations (48), (51), (54), and (81), rather than the first-order equivalent equations (62), (63), (66), (67), (70), (71), (93) and (94).

5.1. *Algebraic system of equations for coefficients in the polynomial approximation*

For each piece p, there are $(m+1)(m+2)/2$ unknown constants in the polynomial approximation of each kernel function $K^{ij}(x,s)$. Thus, for each piece p, there is a total of $n(m+1)(m+2)/2$ unknown constants, corresponding to all the kernels in a given column of the matrix $K(x,s)$; whose values have to be determined. For this purpose, define ${}_pD^j$ as the column vector of dimension $n(m+1)(m+2)/2$ whose elements are the coefficients ${}_pd^{ij}_{ab}$ of the polynomial approximations of all the kernels in a given column $j \in \{1,\dots,n\}$ and a given piece of the domain $p \in \{1,\dots,p^{\max}\}$, arranged in some particular order, for example

$${}_pD^j = \left[{}_pd^{1j}_{00}, {}_pd^{1j}_{10}, {}_pd^{1j}_{01}, \dots, {}_pd^{1j}_{0m}, \dots, {}_pd^{nj}_{0m}\right]^T. \tag{115}$$

The problem of approximating $K(x,s)$ with a *triangular* polynomial of order m is now the problem of finding the values of ${}_pD^j$; for all the columns $j \in \{1,\dots,n\}$ in $K(x,s)$ and for all pieces $p \in \{1,\dots,p^{\max}\}$ of the domain. Each second order hyperbolic equation in (48), (51) or (54) provides $(m-1)m/2$ algebraic equations. To see this, note that the differential operation in the left-hand side of the equations, applied to the polynomial approximation of order m, leads to a $(m-2)$th order polynomial, that is

$$\epsilon_i \frac{\partial_p K^{ij}_m}{\partial x^2}(x,s) - \epsilon_j \frac{\partial_p K^{ij}_m}{\partial s^2}(x,s) = \sum_{a=0}^{m-2}\sum_{b=0}^{m-2-a}\Bigg(\epsilon_i(a+2)(a+1){}_pd^{ij}_{a+2,b} - \epsilon_j(b+2)(b+1){}_pd^{ij}_{a,b+2}\Bigg)x^a s^b. \tag{116}$$

The algebraic operation on the right hand side of the equations in (48), (51) and (54), applied to a $(m-2)$th order polynomial approximation of the kernels, results in a second $(m-2)$th order polynomial

$$c_{jp}K^{ij}_{m-2}(x,s) - \sum_{l=1}^{n}\lambda_{il}(x)_lK^{lj}_{m-2}(x,s) = \sum_{a=0}^{(m-2)}\sum_{b=0}^{(m-2-a)}\left(c_{jp}d^{ij}_{ab} - \sum_{l=1}^{n}\sum_{r=0}^{a}{}_p\lambda^{il}_r{}_pd^{ij}_{a-r,b}\right)x^a s^b, \tag{117}$$

where ${}_p\lambda^{ij}_r \in \mathbb{R}$ are the coefficients of some mth order polynomial approximation of $\lambda_{ij}(x)$; around some point x_0 in the piece p. Since equations in (48), (51) and (54) hold for all points (x,s) in the domain, the coefficients of each power $x^a s^b$ have to coincide for both polynomials in (116) and (117). Thus, for all $a+b \le m-2$, and for all $i \in \{1,2,\dots,n\}$,

$$\epsilon_i(a+2)(a+1){}_pd^{ij}_{a+2,b} - \epsilon_j(b+2)(b+1){}_pd^{ij}_{a,b+2} - c_{jp}d^{ij}_{a,b} - \sum_{l=1}^{n}\sum_{r=0}^{a}{}_p\lambda^{il}_r{}_pd^{ij}_{a-r,b} = 0. \tag{118}$$

These are $n(m-1)m/2$ linear algebraic equations which can be arrange in a nm$(m-1)/2$ by $n(m+2)(m+1)/2$ matrix ${}_pM^j_{\text{PDE}}$; following the order chosen for ${}_pD^j$. Note that $n(2m+1)$ more equations are needed to equate the number of equations and unknowns; these will be provided by boundary and continuity conditions. Since continuity conditions are actually boundary conditions at the boundaries between pieces, there is no need to distinguish between both in the polynomial approximation. Continuity of a kernel function is a Dirichlet-type condition, and continuity of a derivative of a kernel function is a Neumann-type boundary condition. Dirichlet-type conditions provide $m+1$ algebraic equations while Neumann-type conditions provide m algebraic equations. For example, a Neumann-type condition at $x=0$, that is $\partial_{xp}K^{ij}(0,s) = {}_p\alpha_{ij}(s)$, for $s \in (0,1)$, applied to the mth order polynomial approximation ${}_pK^{ij}_m(x,s)$ is

$$\sum_{b=0}^{m-1} a_p d^{ij}_{1b}s^b = \sum_{b=0}^{m-1}{}_p\alpha^{ij}_b s^b, \tag{119}$$

where ${}_p\alpha^{ij}_b$ are the coefficients of some $(m-1)$th order polynomial approximation of ${}_p\alpha_{ij}(s)$; around a point s_0 in the piece p. Eq. (119) is true for all values $s \in (0,1)$, therefore

$$a_p d^{ij}_{1b} = {}_p\alpha^{ij}_b \text{ for all } b \in \{0,\dots,m-1\}. \tag{120}$$

On the other hand, a Dirichlet-type condition at some line of the form $s = m_{\text{slp}}x$, that is ${}_pK^{ij}(x, m_{\text{slp}}x) = {}_p\beta_{ij}(x)$, for $x \in (0,1)$, applied to the mth order polynomial approximation of ${}_pK^{ij}_m(x,s)$, is

$$\sum_{r=0}^{m}\left(\sum_{r=a+b} m^b_{\text{slp}}{}_pd^{ij}_{ab}\right)x^r = \sum_{r=0}^{m}{}_p\beta^{ij}_r x^r, \tag{121}$$

where ${}_p\beta^{ij}_r$ are the coefficients of some polynomial approximation of $\beta_{ij}(x)$; around some point x_0 in the piece p. Eq. (121) holds for all values of $x \in (0,1)$, therefore

$$\sum_{r=a+b} m^b_{\text{slp}}{}_pd^{ij}_{ab} = {}_p\beta^{ij}_r \text{ for all } r \in \{0,\dots,m\}. \tag{122}$$

Together, one Neumann-type and one Dirichlet-type conditions provide $2m+1$ algebraic equations of the form (120) or (122). It is then possible to arrange the $2m+1$ equations for each of the n kernels in a given column $j \in \{1,\dots,n\}$ of $K(x,s)$, for particular piece $p \in \{1,\dots,p^{\max}\}$ of the domain, in a matrix ${}_pM^j_{\text{BC}}$ of dimensions $n(2m+1) \times n(m+2)(m+1)/2$. Thus a system of algebraic equations for ${}_pD^j$ is obtained

$$\left[\frac{{}_pM^j_{\text{PDE}}}{{}_pM^j_{\text{BC}}}\right]{}_pD^j = \left[\begin{array}{c} 0 \\ \hline {}_p\alpha^j \\ {}_p\beta^j \end{array}\right], \tag{123}$$

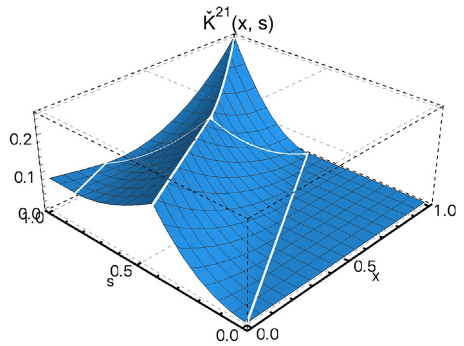

Fig. 8. Piecewise polynomial approximation of the kernel $\check{K}^{21}(x,s)$.

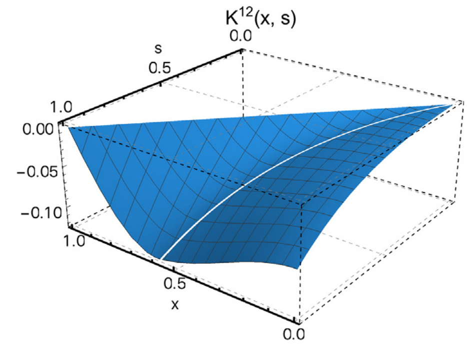

Fig. 9. Piecewise polynomial approximation of the kernel $K^{12}(x,s)$.

where ${}_p\alpha^j$ and ${}_p\beta^j$ are column vectors with elements ${}_p\alpha_b^{ij}$ for $b\in\{0,\dots,m-1\}$, $i\in\{1,\dots,n\}$ and ${}_p\beta_r^{ij}$ for $r\in\{0,\dots,m\}$, $i\in\{1,\dots,n\}$. Note that continuity conditions enforce a particular order. That is, functions ${}_p\alpha^{ij}$ and ${}_p\beta^{ij}$ might actually correspond to a polynomial approximation of $K^{ij}(x,s)$ in a contiguous piece of the domain. Thus, one can either solve the approximation problem sequentially, following this order, or simultaneously for all coefficients in the problem (including those for $\check{K}(x,s)$). The construction of a polynomial approximation for $\check{K}(x,s)$ follows the same approach. In this case, equations are not coupled and therefore, a matrix ${}_p\check{M}^{ij}_{\mathrm{PDE}}$ can be derived for the unknown constants ${}_p\check{d}^{ij}_{ab}$ of a single coefficient of the matrix $\check{K}(x,s)$.

Remark 3. The approximation of $K(x,s)$ and $\check{K}(x,s)$ by polynomials of mth order, requires $\lambda_{ij}(x)\in C^m(0,1)$; in particular, Eqs. (117). This requirement is related to the smoothness of the solutions to the kernel equations. Indeed, following the steps in [13, Theorem A.1], the property $\lambda_{ij}(x)\in C^m(0,1)$ results in solutions $K(x,s)$ and $\check{K}(x,s)$, which are piecewise $C^m(\mathcal{T})$ and $C^m(\mathcal{S})$, respectively.

6. Example

6.1. Kernel functions

For a pair of coupled reaction–diffusion equation, a total of five kernel functions have to be computed. Fig. 8 shows a plot of the polynomial approximation of the non-zero element in the kernel matrix $\check{K}$ and Fig. 9 shows a plot of the polynomial approximation of the element K_{12} The order of polynomial approximation is $m=10$, and the parameters in the problem are the following

$$\Sigma=\begin{bmatrix}1&0\\0&3\end{bmatrix},\ \Lambda(x)=\begin{bmatrix}1&x\\x&1\end{bmatrix},\ C=\begin{bmatrix}5&0\\0&11\end{bmatrix}. \tag{124}$$

6.2. Observer

To evaluate the performance of the observer, we consider an unstable pair of coupled diffusion–reaction equations in the form (3)–(6), with parameters Σ and $\Lambda(x)$ in (124), together with

$$A=\frac{1}{10}\begin{bmatrix}1&1\\1&1\end{bmatrix},\ f(t)=\begin{bmatrix}0\\0\end{bmatrix}. \tag{125}$$

Functions $g_1(t)$ and $g_2(t)$ are chosen as piecewise constant functions taking values from the set $\{-10,0,10\}$. The evolution of the second state $u_2(x,t)$, for a particular choice of non-zero initial conditions, is shown in Fig. 10. The observer for this example has the form (7)–(8), where gains P and Q are computed from (13); with the matrix B set to zero and the matrix C chosen in (124). To find P and Q we used the numerical approximation of $K(x,s)$ computed previously in Section 6.1. The evolution of the estimation error of the second state, i.e., $\widetilde{u}_2(x,t)$, is shown in Fig. 11.

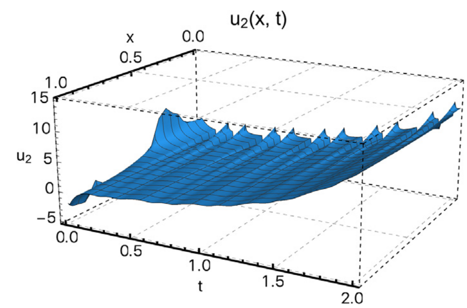

Fig. 10. Evolution of the second state $u_2(x,t)$.

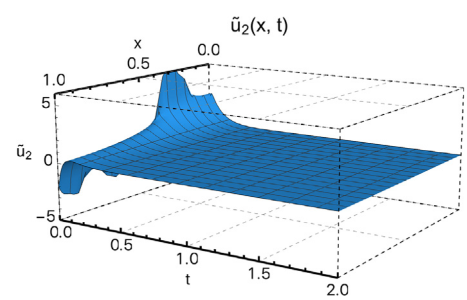

Fig. 11. Estimation error $\tilde{u}_2(x,t)$ for the second state.

7. Conclusion

This paper details the design of observers for coupled systems of diffusion–reaction equations. The converge of the estimate follows from the stability of the estimation error system; derived by mapping the estimation error system to a stable target system using a pair of integral transformations. The target system is a set of n decoupled equations. The simple target system is advantageous to precisely assign designer-chosen convergence rates. Future work includes the adaptive estimation problem, robustness with respect to disturbances, and the use of polynomial approximations as a numerical method for kernel equations arising in the estimation and stabilization problems for other classes of PDEs.

Declaration of competing interest

The authors declare that they have no known competing financial interests or personal relationships that could have appeared to influence the work reported in this paper.

Acknowledgments

Leobardo Camacho-Solorio acknowledges financial support from UC MEXUS, United States of America and CONACYT, Mexico.

References

[1] M. Krstic, A. Smyshlyaev, Boundary Control of PDEs, Society of Industrial and Applied Mathematics, 2008.
[2] A. Baccoli, Y. Orlov, A. Pisano, On the boundary control of coupled reaction–diffusion equations having the same diffusivity parameters, in: Proceedings of the 53rd IEEE Conference on Decision and Control, 2014.
[3] A. Baccoli, A. Pisano, Anticollocated backstepping observer design for a class of coupled reaction–diffusion PDEs, J. Control Sci. Eng. (2015) 53–63.
[4] A. Pisano, A. Baccoli, Y. Orlov, E. Usai, Boundary control of coupled reaction-advection-diffusion equations having the same diffusivity parameter, in: 2nd IFAC Workshop on Control of Systems Governed by Partial Differential Equations, 2016.
[5] A. Baccoli, A. Pisano, Y. Orlov, Boundary control of coupled reaction–diffusion processes with constant parameters, Automatica 54 (2015) 80–90.
[6] Y. Orlov, A. Pisano, A. Pilloni, E. Usai, Output feedback stabilization of coupled reaction–diffusion processes with constant parameters, SIAM J. Control Optim. 55 (2017) 4112–4155.
[7] R. Vazquez, M. Krstic, Boundary control of coupled reaction–diffusion systems with spatially-varying reaction, in: 2nd IFAC Workshop on Control of Systems Governed by Partial Differential Equations, 2016.
[8] L. Camacho-Solorio, R. Vazquez, M. Krstic, Boundary observer design for coupled reaction–diffusion systems with spatially-varying reaction, in: Proceedings of the American Control Conference, 2017.
[9] R. Vazquez, M. Krstic, Boundary control of coupled reaction-advection-diffusion systems with spatially-varying coefficients, IEEE Trans. Automat. Control 62 (4) (2016) 2026–2033.
[10] J. Deutscher, S. Kerschbaum, Backstepping control of coupled linear parabolic PIDEs with spatially-varying coefficients, IEEE Trans. Automat. Control (2018).
[11] J. Deutscher, S. Kerschbaum, Output regulation for coupled linear parabolic PIDEs, Automatica 100 (2019) 360–370.
[12] J. Li, Y. Liu, Adaptive stabilisation for a class of uncertain coupled parabolic equations, Internat. J. Control (2019) 1–11.
[13] L. Hu, R. Vazquez, F. Di Meglio, M. Krstic, Boundary exponential stabilization of 1-D inhomogeneous quasilinear hyperbolic systems, 2015, arXiv preprint, available at http://arxiv.org/abs/1512.03539.
[14] L. Hu, F. Di Meglio, R. Vazquez, M. Krstic, Control of homodirectional and general heterodirectional linear coupled hyperbolic PDEs, IEEE Trans. Automat. Control 61 (2016) 3301–3314.
[15] J. Auriol, F. Di Meglio, Minimum time control of heterodirectional linear coupled hyperbolic PDEs, Automatica 71 (2016) 300–307.
[16] J.-M. Coron, L. Hu, G. Olive, Finite-time boundary stabilization of general linear hyperbolic balance laws via Fredholm backstepping transformation, Automatica 84 (2017) 95–100.
[17] H. Shim, D. Liberzon, Nonlinear observers robust to measurement disturbances in an ISS sense, IEEE Trans. Automat. Control 61 (1) (2016) 48–61.
[18] P. Ascencio, A. Astolfi, T. Parisini, Backstepping PDE design: a convex optimization approach, IEEE Trans. Automat. Control 63 (2017) 1943–1958.
[19] L.C. Evans, Partial Differential Equations, American Mathematical Society, 2010.
[20] S. Drew, B. Gharesifard, A.-R. Mansouri, Controllability of coupled parabolic systems with multiple underactuation, in: Proceedings of the 57th IEEE Conference on Decision and Control, 2018.